

# The preventive effect of loganin on oxidative stress-induced cellular damage in human keratinocyte HaCaT cells

Cheol Park<sup>1</sup>, Hyesook Lee<sup>2</sup>, Soojung Jin<sup>3</sup>, Jung-Ha Park<sup>3,4</sup>, Min Ho Han<sup>5</sup>, Jin-Woo Jeong<sup>6</sup>, Hyun Ju Kwon<sup>3,4</sup>, Byung Woo Kim<sup>3,4</sup>, Shin-Hyung Park<sup>7</sup>, Su Hyun Hong<sup>8,9</sup>, Gi-Young Kim<sup>10</sup>, Yung Hyun Choi<sup>3,8,9,\*</sup>

<sup>1</sup> Division of Basic Sciences, College of Liberal Studies, Dong-eui University, Busan, Korea;

<sup>2</sup> Department of Convergence Medicine, Pusan National University School of Medicine, Yangsan, Korea;

<sup>3</sup> Core-Facility Center for Tissue Regeneration, Dong-eui University, Busan, Korea;

<sup>4</sup> Biopharmaceutical Engineering Major, Division of Applied Bioengineering, College of Engineering, Dong-eui University, Busan, Korea;

<sup>5</sup> National Marine Biodiversity Institute of Korea, Seocheon, Korea;

<sup>6</sup> Nakdonggang National Institute of Biological Resources, Sangju, Korea;

<sup>7</sup> Department of Pathology, Dong-eui University College of Korean Medicine, Busan, Korea;

<sup>8</sup> Anti-Aging Research Center, Dong-eui University, Busan, Korea;

<sup>9</sup> Department of Biochemistry, Dong-eui University College of Korean Medicine, Busan, Korea;

<sup>10</sup> Department of Marine Life Science, Jeju National University, Jeju, Korea.

**SUMMARY** Loganin is a type of iridoid glycosides isolated from *Corni fructus* and is known to have various pharmacological properties, but studies on its antioxidant activity are still lacking. Therefore, in this study, the preventive effect of loganin on oxidative stress-mediated cellular damage in human keratinocyte HaCaT cells was investigated. Our results show that loganin pretreatment in a non-toxic concentration range significantly improved cell survival in hydrogen peroxide (H<sub>2</sub>O<sub>2</sub>)-treated HaCaT cells, which was associated with inhibition of cell cycle arrest at the G2/M phase and induction of apoptosis. H<sub>2</sub>O<sub>2</sub>-induced DNA damage and reactive oxygen species (ROS) generation were also greatly reduced in the presence of loganin. Moreover, H<sub>2</sub>O<sub>2</sub> treatment enhanced the cytoplasmic release of cytochrome *c*, upregulation of the Bax/Bcl-2 ratio and degradation of cleavage of poly (ADP-ribose) polymerase, whereas loganin remarkably suppressed these changes. In addition, loganin obviously attenuated H<sub>2</sub>O<sub>2</sub>-induced autophagy while inhibiting the increased accumulation of autophagosome proteins, including as microtubule-associated protein 1 light chain 3-II and Beclin-1, and p62, an autophagy substrate protein, in H<sub>2</sub>O<sub>2</sub>-treated cells. In conclusion, our current results suggests that loganin could protect HaCaT keratinocytes from H<sub>2</sub>O<sub>2</sub>-induced cellular injury by inhibiting mitochondrial dysfunction, autophagy and apoptosis. This finding indicates the applicability of loganin in the prevention and treatment of skin diseases caused by oxidative damage.

**Keywords** Loganin, ROS, DNA damage, apoptosis, autophagy

## 1. Introduction

*Corni fructus*, a fruit of *Cornus officinalis* Sieb. et Zucc. belonging to the Cornaceae family, has been widely used in East Asia including Korea for the purpose of tonifying the kidneys and liver (1-3). Secondary metabolites, including iridoids, are abundantly present in *Corni fructus*, and studies on the various pharmacological effects of these substances are increasing (3-5). Among them, loganin is an iridoid glycoside compound found and has been reported to have various beneficial effects, including anti-inflammatory, neuroprotective, inhibiting

cartilage degeneration and osteoarthritis, renal protection and improving intestinal function (6-12). These pharmacological activities of loganin are believed to be at least related to its antioxidant effect. For example, loganin protected against hydrogen peroxide (H<sub>2</sub>O<sub>2</sub>) and amyloid- $\beta$ -induced neurotoxicity while inhibiting the production of reactive oxygen species (ROS) (13,14), suggesting that its antioxidant effect was closely associated with ROS scavenging activity. In addition, this compound suppressed diabetes mellitus-induced reproductive damage by restoring glutathione level and superoxide dismutase activity, as well as reducing

ROS level (15). Recently, Wen *et al.* (9) reported that loganin reduced burn-induced intestinal inflammation and oxidative stress, and Cheng *et al.* (16) found that inhibition of NLRP3 inflammasome activation by the antioxidant activity of loganin contributed to the blockade of Schwann cell pyroptosis. Moreover, Xu *et al.* (12) have been reported that the antioxidant activity of loganin contributes to neuronal survival by inhibiting autophagy and mitochondrial division. Similar to these results, we also demonstrated that loganin may be a substance capable of preventing inflammatory and oxidative damage in lipopolysaccharide-stimulated macrophages (17).

Although ROS play an important role as a second messenger during normal cellular metabolism, excessive production of ROS results in progressive oxidative damage to organelles [18, 19]. In particular, ROS act as regulators of body homeostasis, including epidermal keratinocyte proliferation, exacerbating skin aging and has been implicated in various skin diseases (20,21). As in other tissues, oxidative stress caused by excessive accumulation of ROS in keratinocytes ultimately induces depolarization of the mitochondrial membrane potential (MMP,  $\Delta\psi_m$ ), a hallmark of mitochondrial dysfunction. Subsequently, cytochrome *c* is released from the mitochondria into the cytoplasm, which activates the caspase cascade and ultimately induces apoptosis (22,23). More recently, Liu *et al.* (24) suggested that catalpol, a type of natural iridoid glucoside, may have therapeutic properties for psoriasis by ameliorating oxidative stress in tumor necrosis factor- $\alpha$ -stimulated keratinocytes. In addition, natural iridoid glucoside derivatives such as geniposide and aucubin have been reported to have protective effects on oxidative stress induced by ultraviolet-B irradiation in human skin fibroblasts (25,26). However, since the beneficial effect of loganin on epidermal keratinocytes has not been clearly elucidated, in this study, the protective potential of loganin against H<sub>2</sub>O<sub>2</sub>-induced oxidative stress in human keratinocyte HaCaT cells was investigated.

## 2. Materials and Methods

### 2.1. Cell culture and treatment

HaCaT keratinocytes purchased from the American Type Culture Collection (CRL-1458™, Manassas, VA, USA) were cultured in Dulbecco's modified Eagle's medium containing 10% fetal bovine serum and 1% antibiotics at 37°C and 5% CO<sub>2</sub>. All materials needed for cell culture were obtained from WelGENE Inc. (Gyungsan, Korea). Loganin and H<sub>2</sub>O<sub>2</sub> (Sigma-Aldrich Chemical Co., St. Louis, MO, USA) were dissolved in dimethyl sulfoxide (Thermo Fisher Scientific, Waltham, MA, USA) and distilled water to prepare stock solutions of 100 mM each. The stock solutions were diluted in the medium before utilization.

### 2.2. Cell viability

A 3-(4,5-dimethylthiazol-2-yl)-2,5-diphenyltetrazolium bromide (MTT) assay is used to measure cell viability, as previously described (27). Briefly, HaCaT cells were stimulated with the different concentrations of loganin or H<sub>2</sub>O<sub>2</sub> alone for 24 h, or exposed to loganin for 1 h and then treated with H<sub>2</sub>O<sub>2</sub> for 24 h. At the end time, the MTT reaction was run and absorbance was measured with a microplate reader (Beckman Coulter Inc., Brea, CA, USA) at the Core Facility Center for Tissue Regeneration (Dong-eui University, Busan, Korea). Images of cell morphological changes were captured using an inverted microscope (Carl Zeiss, Oberkochen, Germany).

### 2.3. Cell cycle analysis

For cell cycle analysis of H<sub>2</sub>O<sub>2</sub>-treated or untreated cells with and without loganin for 24 h, both adherent and detached cells were washed with phosphate-buffered saline (PBS) and then fixed by ethanol, as previously described (28). After that, cells were exposed with RNAase and propidium iodide (PI) (Thermo Fisher Scientific, Waltham, MA, USA) for 20 min at 4°C. Cell cycle distributions were calculated after appropriate gating of cell populations using flow cytometry (Becton Dickinson, San Jose, CA, USA).

### 2.4. Apoptosis analysis

To observe whether apoptosis was induced, flow cytometry was performed according to a published method (29). Briefly, cells were stimulated with H<sub>2</sub>O<sub>2</sub> for 24 h with or without loganin, washed with PBS and then fixed with 4% paraformaldehyde solution for 15 min. Subsequently, cells were stained with annexin V-fluorescein isothiocyanate (FITC)/propidium iodide (PI) (Becton Dickinson), and annexin V-positive cells were quantified as cells induced by apoptosis using a flow cytometer.

### 2.5. Analysis of intracellular ROS

To measure the levels of ROS, the collected cells were stained with 2',7'-dichlorofluorescein diacetate (DCF-DA) dye (Sigma-Aldrich Chemical Co.). In brief, treated cells were collected and preloaded with 10  $\mu$ M DCF-DA for 20 min at 37°C in the dark. The fluorescence intensity was observed under a fluorescence microscope as previously described (30). In parallel, ROS generation was quantified using flow cytometry (31). N-acetyl-L-cysteine (NAC, Sigma-Aldrich Chemical Co.) was used as a positive control as a scavenger of ROS.

### 2.6. Comet assay

A comet assay<sup>®</sup> kit obtained from Trevigen, Inc.

(Gaithersburg, MD, USA) was used to evaluate DNA damage according to the manufacturer's kit protocols (32). The localized green fluorescence of apoptotic cells was detected using fluorescent microscope (Leica, Wetzlar, Germany). The stained cells were imaged using a fluorescence microscope.

#### 2.7. Immunofluorescence assay for detection of phospho (p)- $\gamma$ H2AX

To observe intracellular expression of p- $\gamma$ H2AX, a marker of DNA strand breakage (30), cells grown on 4-well chamber slide were stimulated with or without loganin for 1 h and then treated with H<sub>2</sub>O<sub>2</sub> for additional 24 h. After fixing with 4% paraformaldehyde solution at room temperature (RT) for 20 min, cells were incubated with ice-cold PBS containing 1% bovine serum albumin (Sigma-Aldrich Chemical Co.) and 1% Triton X-100 (Sigma-Aldrich Chemical Co.) for 1 h. Subsequently, immunostaining was performed using an antibody against p- $\gamma$ H2AX (Abcam, Inc., Cambridge, UK) at 4°C overnight and then reacted with Alexa Fluor® 647-conjugated secondary antibody (Abcam, Inc.) for 1 h at RT. Additionally, nuclei were also stained with 4',6'-diamidino-2-phenylindole (DAPI) solution (Thermo Fisher Scientific) for 20 min at RT. The cells were immediately observed under a fluorescence microscope (Carl Zeiss).

#### 2.8. Western blotting for protein expression analysis

Whole cell lysates for immunoblotting were prepared according to a previous method (33). To isolate the cytoplasmic and mitochondrial fractions, a mitochondrial/cytoplasmic fractionation kit (Active Motif, Inc., Carlsbad, CA, USA) was used. For Western blot analysis, the same amount of protein for each treatment group was separated by sodium dodecyl sulfate-polyacrylamide gel electrophoresis and transferred to polyvinylidene difluoride membranes, and then the primary antibodies purchased from Santa Cruz Biotechnology, Inc. (Santa Cruz, CA, USA), Abcam, Inc.), Thermo Fisher Scientific and Cell Signaling Technology (Danvers, MA, USA) were probed, as previously described (34). Subsequently, the membranes that had finished reacting with the primary antibodies reacted with the correlated secondary antibodies (Santa Cruz Biotechnology, Inc.). The membranes were then exposed enhanced chemiluminescence solution (Thermo Fisher Scientific) and visualized using a Fusion FX Imaging System (Vilber Lourmat, Torcy, France). Band intensities were quantified and normalized to a loading control by densitometry using ImageJ® software (v1.48, National Institutes of Health, Bethesda, MD, USA).

#### 2.9. MMP assay

To measure MMP, the cells were stained with 5,5',6,6'-tetrachloro-1,1',3,3'-tetraethylimidocarbocyanine iodide (JC-1, Thermo Fisher Scientific) reagent according to the previous methods (35,36), and quantitative analysis was performed using a flow cytometer, and fluorescence images were taken with a fluorescence microscope.

#### 2.10. Autophagic activity detection

To evaluate the occurrence of autophagy, the Cyto-ID® Autophagy Detection Kit (Enzo Life Sciences Inc, Farmingdale, NY, USA) was employed according to the manufacturer's instructions. In brief, the treated cells were collected, suspended, stained with the Cyto-ID staining solution provided in the kit at RT temperature in the dark, and then autophagy-induced cells were quantitatively analyzed using flow cytometry (36). In parallel with this, DAPI staining was used to counterstain the nuclei, and localized green fluorescence of autophagic cells was detected under a fluorescence microscope (30).

#### 2.11. Statistical analysis

All experiments were independently repeated at least 3 times to determine significance. Results were presented as mean and standard deviation (SD) using SPSS 25.0 (SPSS Inc., Chicago, IL, USA), and differences ( $p < 0.05$ ) were considered statistically using ANOVA-Tukey's post-hoc test.

### 3. Results

#### 3.1. Loganin prevented the loss of HaCaT cell viability caused by H<sub>2</sub>O<sub>2</sub> treatment

As indicated in Figure 1A, loganin has been no cytotoxicity up to 12.5  $\mu$ M of concentration in HaCaT cells. However, cells exposed to 15  $\mu$ M loganin showed a slight inhibition in cell viability. Therefore, 12.5  $\mu$ M was selected the maximum concentration of loganin to establish its efficacy, we performed further experiments. The cell viability in HaCaT cells treated with 500  $\mu$ M H<sub>2</sub>O<sub>2</sub> was significantly reduced to approximately 60% compared that in the untreated control cells (Figure 1B). However, pretreatment of loganin significantly inhibited H<sub>2</sub>O<sub>2</sub>-induced reduction of cell viability in a concentration-dependent manner (Figure 1C). Especially, exposure to NAC as a positive control restored cell viability that could control the level of H<sub>2</sub>O<sub>2</sub>-stimulated cells. In addition, morphological alterations such as cell shrinkage and cytoplasm vacuolization were observed in H<sub>2</sub>O<sub>2</sub>-treated cells, but not in the presence of loganin (Figure 1D).

#### 3.2. Loganin restored cell cycle arrest and apoptotic cell death in H<sub>2</sub>O<sub>2</sub>-treated HaCaT cells

As shown in Figure 2A, the population of cells belonging to the G2/M phase in H<sub>2</sub>O<sub>2</sub>-treated HaCaT cells was significantly increased compared to the untreated control group, which was attenuated by loganin pretreatment. The proportion of cells with sub-G1 DNA content,

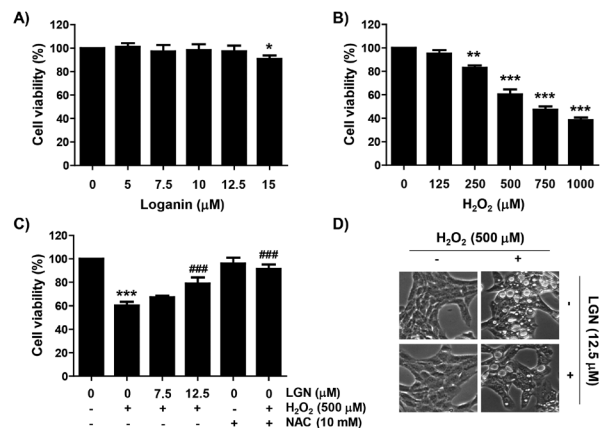


**Figure 1. Inhibitory effects of loganin on H<sub>2</sub>O<sub>2</sub>-mediated cytotoxicity in HaCaT cells.** Cells were treated with different concentrations of loganin (LGN) or H<sub>2</sub>O<sub>2</sub> for 24 h (A and B) or treated the indicated concentrations of loganin or NAC (10 mM) for 1 h, and then stimulated with H<sub>2</sub>O<sub>2</sub> for 24 h (C and D). (A-C) The results of quantitative analysis of cell viability according to MTT assay were presented. The data were represented as mean ± SD of three independent experiments. Significant differences compared to the control cells (<sup>\*</sup>*p* < 0.05, <sup>\*\*</sup>*p* < 0.01 and <sup>\*\*\*</sup>*p* < 0.001) or H<sub>2</sub>O<sub>2</sub>-treated cells (<sup>###</sup>*p* < 0.001) were shown. (D) Representative cell morphologies observed under an inverted microscope are presented.

which indicates the frequency of apoptosis, also greatly increased after H<sub>2</sub>O<sub>2</sub> treatment compared with control cells, which significantly diminished by pretreatment of loganin (Figure 2A and 2B). In addition, the population of annexin V-positive cells was also significantly increased in H<sub>2</sub>O<sub>2</sub>-treated HaCaT cells (Figure 2C and 2D), which was markedly suppressed by loganin pretreatment. The results indicate that, similar to the NAC pretreatment group, loganin substantially attenuated cell cycle arrest and apoptotic cell death following by H<sub>2</sub>O<sub>2</sub>, thereby restoring cell viability.

### 3.3. Loganin inhibited ROS production in H<sub>2</sub>O<sub>2</sub>-stimulated HaCaT cells

The results of flow cytometry after DCF-DA staining showed that the level of intracellular ROS production was markedly increased in H<sub>2</sub>O<sub>2</sub>-exposed HaCaT cells (Figure 3A and 3B). Consistent with this result, the DCF-fluorescence image in H<sub>2</sub>O<sub>2</sub>-treated cells was markedly increased compared to that of control cells (Figure 3C). However, similar to NAC pretreatment, loganin significantly decreased H<sub>2</sub>O<sub>2</sub>-induced ROS generation, indicating that the inhibitory effect of loganin on the cytotoxicity of H<sub>2</sub>O<sub>2</sub> in HaCaT cells was related to its antioxidant activity.

### 3.4. Loganin suppressed DNA damage in H<sub>2</sub>O<sub>2</sub>-treated HaCaT cells

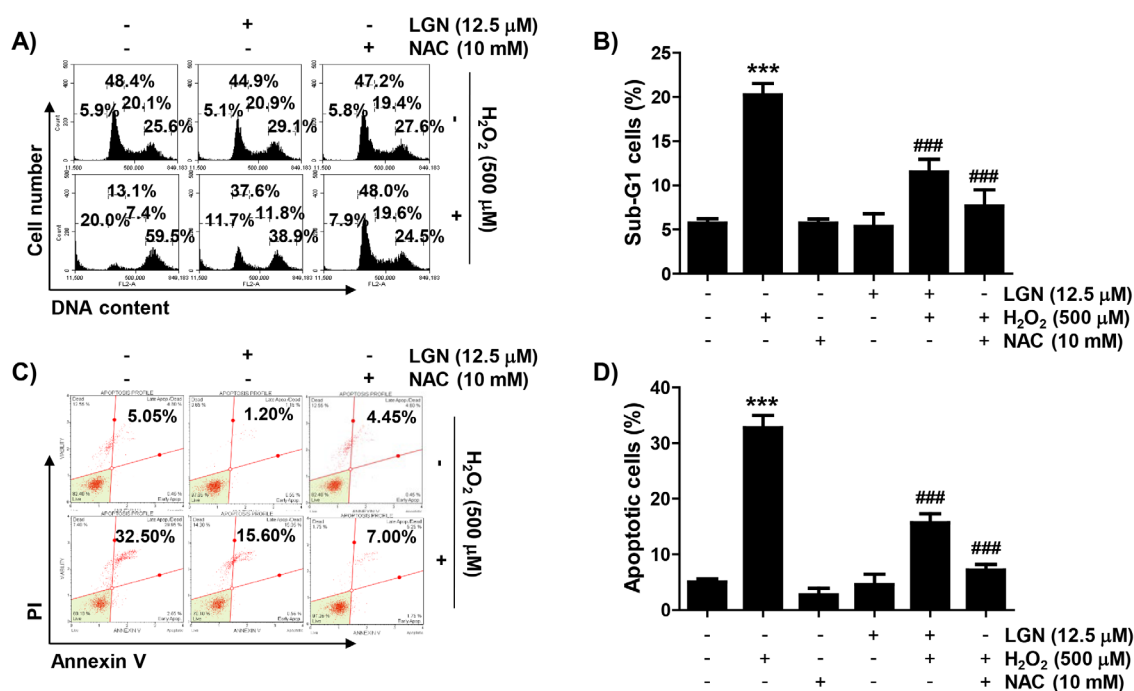


**Figure 2. Attenuation of cell cycle arrest and apoptosis by loganin in H<sub>2</sub>O<sub>2</sub>-treated HaCaT cells.** Cells were incubated in medium containing loganin (12.5 μM) or NAC (10 mM) for 1 h, and then exposed to H<sub>2</sub>O<sub>2</sub> (500 μM) for 24 h. (A and B) Cells were collected and analysis of cell cycle distribution was performed. (A) Representative flow histograms were presented. (B) The frequency of sub-G1 cells were presented. (C and D) Cells were stained with annexin V-FITC/PI, and analyzed by flow cytometry. (C) The population of apoptotic cells were shown in the upper right panel of representative histograms. (D) The averages of the frequencies of apoptotic cells were presented. (B and D) The data were represented as mean ± SD of three independent experiments. Significant differences compared to the control cells (<sup>\*</sup>*p* < 0.001) or H<sub>2</sub>O<sub>2</sub>-treated cells (<sup>###</sup>*p* < 0.001) were shown.

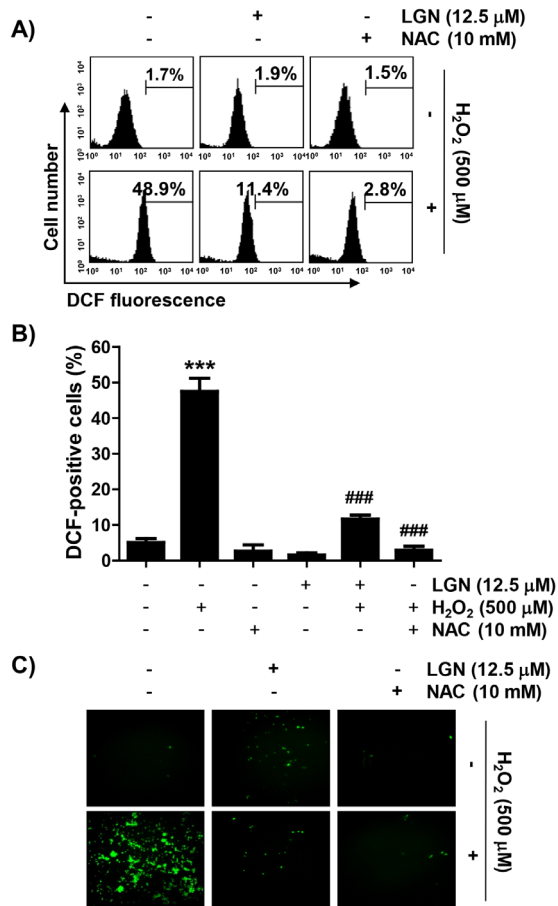


**Figure 3. Inhibitory effects of loganin on ROS generated by H<sub>2</sub>O<sub>2</sub> in HaCaT cells.** Cells were cultured in medium containing loganin (12.5 μM) or NAC (10 mM) for 1 h, treated with H<sub>2</sub>O<sub>2</sub> (500 μM) for 1 h and stained with DCF-DA. (A and B) Intracellular ROS levels were calculated using a flow cytometer (A and B) or observed under a fluorescence microscope (C). (B) Significant differences compared to the control cells (\*\*p < 0.001) or H<sub>2</sub>O<sub>2</sub>-treated cells (###p < 0.001) were shown.

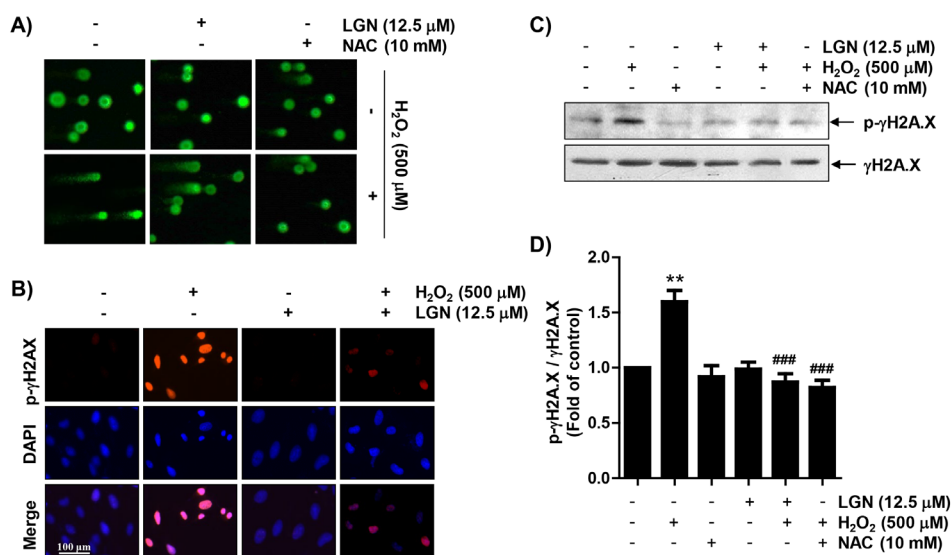


**Figure 4. Inhibition of DNA damage by loganin in H<sub>2</sub>O<sub>2</sub>-treated HaCaT cells.** Cells were stimulated with loganin (12.5 μM) or NAC (10 mM) for 1 h, and then exposed to H<sub>2</sub>O<sub>2</sub> (500 μM) for 24 h. (A) Representative images of comet assay were shown. (B) Cells exposed to the indicated treatments were labeled for p-γH2AX (red) and DAPI (blue), and representative immunofluorescence images are presented. (C) The protein expression of p-γH2AX was investigated using Western blotting. Actin was used as the reference. (D) The relative expression levels of p-γH2AX protein were quantified by densitometry. Significant differences compared to the control cells (\*p < 0.01) or H<sub>2</sub>O<sub>2</sub>-treated cells (###p < 0.001) were shown.

Next, we investigated the inhibitory effect of loganin on DNA damage induced by H<sub>2</sub>O<sub>2</sub>-treatment. According to the comet assay results, DNA tails caused by damaged DNA fragments were markedly enhanced in H<sub>2</sub>O<sub>2</sub>-treated HaCaT cells (Figure 4A). However, these tails were markedly reduced in cells pretreated with loganin and NAC. Immunofluorescence indicated that H<sub>2</sub>O<sub>2</sub> significantly increased the number of p-γH2AX positive-stained nuclei compared to control cells (Figure 4B). In addition, the expression of p-γH2A.X protein was strongly enhanced in H<sub>2</sub>O<sub>2</sub>-treated cells (Figure 4C and 4D). However, its expression was attenuated by loganin pretreatment, indicating that the inhibitory effect of loganin against H<sub>2</sub>O<sub>2</sub>-induced DNA damage was related to inhibition of ROS generation.

### 3.5. Loganin alleviated the change of apoptosis regulators expression in H<sub>2</sub>O<sub>2</sub>-treated HaCaT cells

As indicated in Figure 5A and 5B, the protein level of Bax was up-regulated in H<sub>2</sub>O<sub>2</sub>-treated HaCaT cells, while that of Bcl-2 was down-regulated. In addition, H<sub>2</sub>O<sub>2</sub> enhanced the degradation of poly (ADP-ribose) polymerase (PARP). Furthermore, the level of cytochrome *c* expression in the mitochondria of cells treated with H<sub>2</sub>O<sub>2</sub> was decreased, but its expression in the cytoplasm was increased (Figure 5C and 5D), which was associated with loss of MMP (Figure 5E and 5F). However, H<sub>2</sub>O<sub>2</sub>-induced these alterations were remarkably suppressed with loganin pretreatment, indicating that loganin protected HaCaT cells from apoptosis by blocking mitochondrial damage caused by H<sub>2</sub>O<sub>2</sub>.

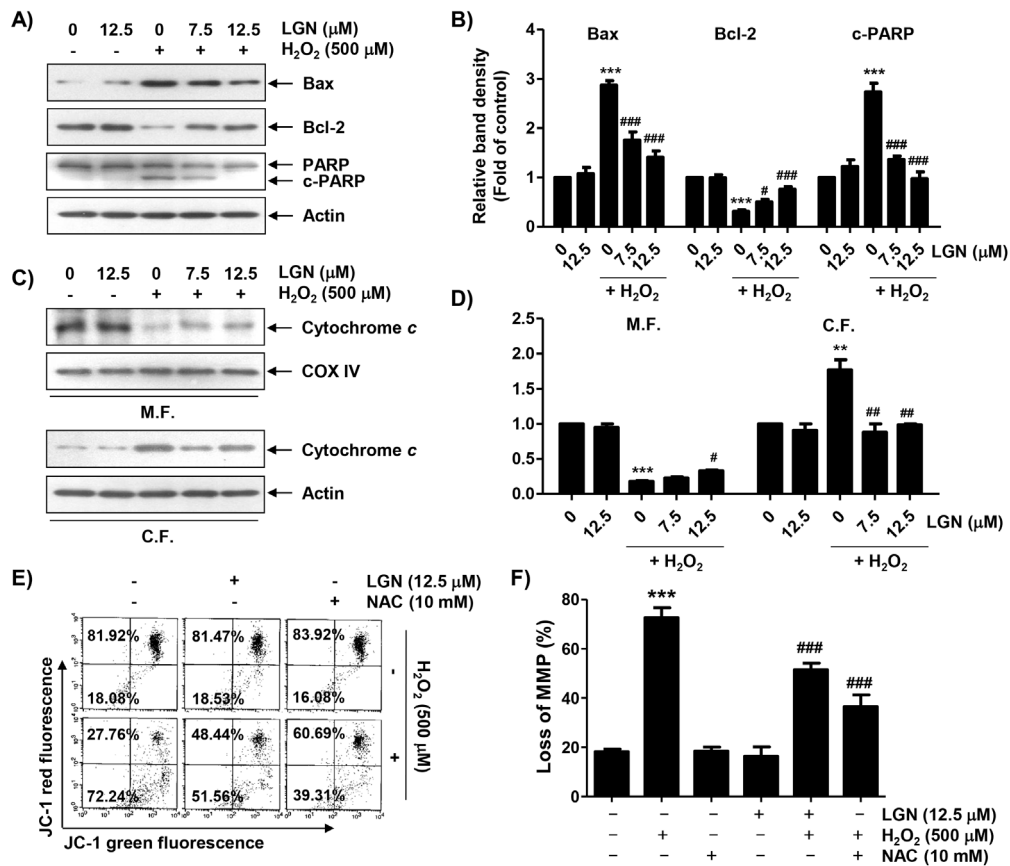


**Figure 5. Inhibitory effect of loganin on changes of mitochondria-mediated apoptosis regulatory factors in H<sub>2</sub>O<sub>2</sub>-treated HaCaT cells.** Cells were pretreated with loganin (12.5 μM) for 1 h, and then incubated with H<sub>2</sub>O<sub>2</sub> (500 μM) for additional 24 h. (A) Protein expression of apoptosis-related mediators was investigated using total proteins. Actin was used as an internal standard. (C) Expression of cytochrome *c* in mitochondrial and cytoplasmic fractions was investigated. Actin and cytochrome *c* oxidase subunit IV (COX IV) were used as the reference genes for cytosolic and mitochondrial fractions (M.F., mitochondrial fraction; C.F., cytoplasmic fraction). (B and D) The relative expression levels of Bax, Bcl-2, c-PARP and cytochrome *c* protein were quantified by densitometry. (E and F) MMPs were examined by flow cytometry after JC-1 staining. (E) Representative profiles of flow cytometry analysis were presented. (F) Ratios of JC-1 aggregates to monomers were presented as mean ± SD of triplicate independent experiments. Significant differences compared to the control cells (\*\**p* < 0.01 and \*\*\**p* < 0.001) or H<sub>2</sub>O<sub>2</sub>-treated cells (#*p* < 0.05, ##*p* < 0.01 and ###*p* < 0.001) were shown.

### 3.6. Loganin attenuates H<sub>2</sub>O<sub>2</sub>-induced autophagy in HaCaT cells

Since the formation of autophagic vacuoles, which is typical of autophagy induction, was increased in H<sub>2</sub>O<sub>2</sub>-treated HaCaT cells (Figure 1D), we investigated whether autophagy was induced by H<sub>2</sub>O<sub>2</sub> and whether loganin could inhibit it. The results of flow cytometry using Cyto-ID staining showed that autophagy was definitely induced in the cells treated with H<sub>2</sub>O<sub>2</sub>, as shown in Figure 6A and 6B, which was greatly reduced in the presence of loganin, and the same results were observed in the results of fluorescence microscopy (Figure 6C). Subsequently we detected autophagy biomarkers using Western blot analysis to confirm H<sub>2</sub>O<sub>2</sub>-induced autophagy, and found that H<sub>2</sub>O<sub>2</sub> increased the accumulation of proteins such as microtubule-associated protein 1 light chain 3 (LC3)-II, beclin-1 and p62 (Figure 6D and 6E). However, their expression was obviously attenuated when loganin and H<sub>2</sub>O<sub>2</sub> were treated together, suggesting that autophagy inhibition was implicated in the protection of HaCaT cells by loganin from oxidative damage caused by H<sub>2</sub>O<sub>2</sub>.

## 4. Discussion

In this study, we examined the efficacy of loganin on oxidative damage in H<sub>2</sub>O<sub>2</sub>-stimulated HaCaT keratinocytes. Our finding indicated that loganin significantly inhibited H<sub>2</sub>O<sub>2</sub>-induced cellular dysfunctions, including cell cycle arrest at the G2/M phase, DNA damage and apoptotic cell death, which was caused by blocking of ROS accumulation. Furthermore, we showed that the antioxidant potential of loganin was accompanied by inhibition of autophagy H<sub>2</sub>O<sub>2</sub>-treated HaCaT cells.

As is well known, H<sub>2</sub>O<sub>2</sub>, as oxidative stressor, induce cell cycle arrest at the G2/M phase in most cells, including keratinocytes, causing to DNA damage as well as cell death (37-39). In this study, reduction of cell survival in H<sub>2</sub>O<sub>2</sub>-treated HaCaT cells was accompanied by inhibition of cell cycle progression at the G2/M phase, which was in good agreement with the previous findings (38,40). However, these effects were significantly inhibited by loganin pretreatment. We also demonstrated that, in good agreement with previous studies (9,13-17),

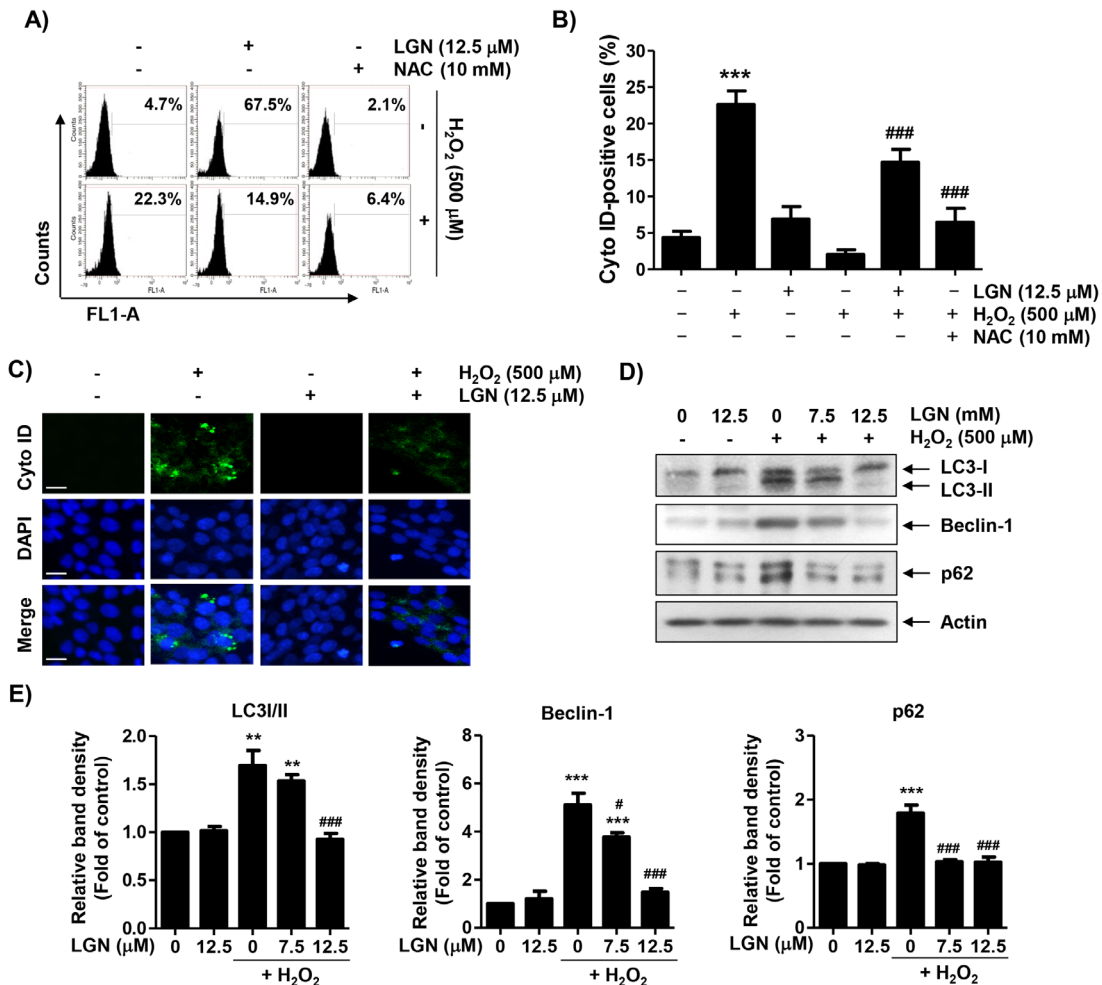


**Figure 6. Protection of H<sub>2</sub>O<sub>2</sub>-induced autophagy by loganin in HaCaT cells.** Cells were incubated with loganin (12.5 μM) or NAC (10 mM) for 1 h, and then incubated with H<sub>2</sub>O<sub>2</sub> (500 μM) for additional 24 h. (A and B) Cells were stained with Cyto-ID, and analyzed by flow cytometry. (A) The frequency of autophagic cells were shown in the upper right panel of representative histograms. (B) The averages of the frequencies of autophagic cells were presented. (C) Cells were labeled for Cyto-ID (green) and DAPI (blue), and representative immunofluorescence images are presented. (D) Protein expression of autophagy-regulatory proteins was determined using total proteins. Actin was used as an internal standard. (E) The relative expression levels of LC3, Beclin-1 and p62 protein were quantified by densitometry. Significant differences compared to the control cells (\*\**p* < 0.01 and \*\*\**p* < 0.001) or H<sub>2</sub>O<sub>2</sub>-treated cells (\**p* < 0.05, \*\**p* < 0.01 and \*\*\**p* < 0.001) were shown.

loganin had potent antioxidant activity by significantly inhibiting H<sub>2</sub>O<sub>2</sub>-induced ROS generation. Oxidative stress induces damage to intracellular macromolecules such as nucleic acids, contributing to DNA damage and apoptosis (41,42). The results of the comet assay, a commonly used method to measure DNA strand breaks (43), showed that loganin largely blocked H<sub>2</sub>O<sub>2</sub>-induced comet tail formation. Additionally, in the immunoblotting results for analyzing the phosphorylation level of γH2AX (p-γH2AX), which indicates that the DNA double-strand is broken by oxidative stress (33), enhanced expression of p-γH2AX by H<sub>2</sub>O<sub>2</sub> was effectively suppressed in the presence of loganin. These findings demonstrated that loganin has a remarkable ameliorating effect for H<sub>2</sub>O<sub>2</sub>-triggered DNA damage in HaCaT keratinocytes.

According to the results of previous studies, H<sub>2</sub>O<sub>2</sub>-induced apoptosis in HaCaT cells was strongly correlated with the cytosolic release of apoptogenic factors, including cytochrome *c*, which initiates the mitochondria-mediated intrinsic apoptosis pathway

(40,44,45). Cytochrome *c* released into the cytoplasm following the loss of MMP activates effector caspases such as caspase-3 and -7 through the activation of caspase-9, which induce degradation of matrix proteins including PARP to terminate apoptosis (46,47). In this study, the expression of cytochrome *c* was up-regulated in the cytoplasm and the loss of MMP was increased in H<sub>2</sub>O<sub>2</sub>-treated cells, consistent with previous studies (40,44). However, the expression of cytochrome *c* in the cytoplasm and mitochondria and the level of MMP were maintained at control levels in loganin-pretreated cells, suggesting that mitochondrial integrity in H<sub>2</sub>O<sub>2</sub>-treated HaCaT cells was maintained in the presence of loganin. Subsequently, the increase of Bax/Bcl-2 ratio by H<sub>2</sub>O<sub>2</sub> was also counteracted by loganin pretreatment, which was correlated with to suppressing the cleavage of PARP. Bcl-2 family members control the release of apoptogenic factors through regulation of mitochondrial membrane permeability (46,47). Therefore, it is presumed that the reduction of the Bax/Bcl-2 expression ratio by loganin

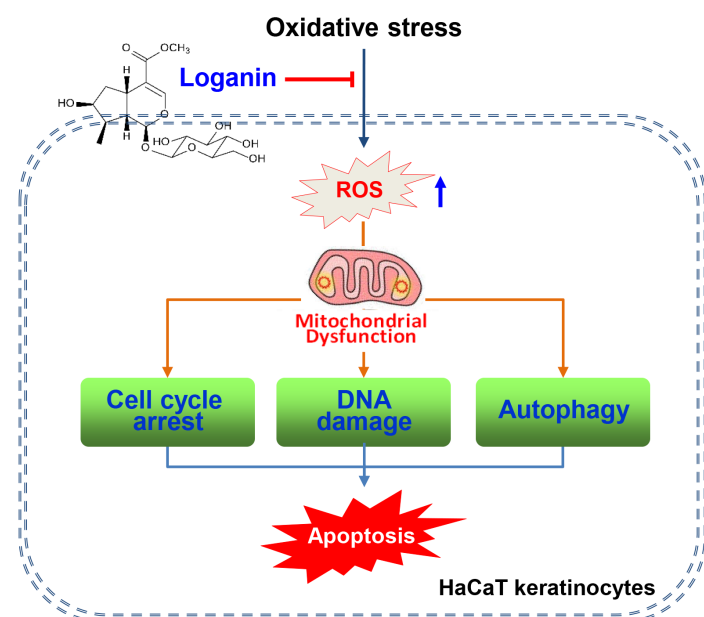


Figure 7. Schematic diagram representing the protective mechanism of loganin against oxidative damage in HaCaT cells.

plays a critical role in attenuating  $H_2O_2$ -induced HaCaT cell apoptosis. Based on this finding, we considered that loganin might be a potential antioxidant that prevents mitochondrial-dependent apoptosis as a scavenger of ROS. Our results agree very well with the results of Kwon *et al.* (14) on the blocking effect of loganin on the induction of apoptosis by  $H_2O_2$  in SH-SY5Y neuronal cells.

Cellular damage, including DNA damage and apoptosis due to oxidative stress, is often accompanied by autophagy (48,49). In keratinocytes, it has also been reported that autophagy is involved in DNA damage and apoptosis caused by oxidative stress inducers (50,51), suggesting that ROS are potent and effective triggers of autophagy. Autophagy is a highly conserved self-digestion process for recycling cytoplasmic components such as unwanted protein aggregates and damaged organelles, which are sequestered into newly generated double-membraned structures called autophagosomes (52,53). Autophagosomes fuse sequentially with lysosomes and are eliminated through lysosomal degradation (54,55). Several important proteins are involved in this process, including LC3-II, Beclin-1 and p62. LC-3, an autophagosome membrane protein, controls key steps in the autophagic pathway, such as autophagic membrane growth and lysosome fusing, and the ratio LC3-II/LC3-I is commonly used to reflect autophagosome formation (52,56). Beclin-1 is involved in the initiation of autophagy by mediating the localization of autophagy proteins into the pre-autophagosomal membrane. In addition, Beclin-1 may be importantly involved in the regulation of apoptosis as well as autophagy because pro-autophagy properties may be reduced by Bcl-2 (57,58). p62 is another autophagosome-lysosomal membrane-associated protein that serves as an autophagic substrate (59,60). Therefore, these proteins are important markers of autophagy flux and critical regulators of autophagy regulation. The flow

cytometry results of this study showed that the frequency of autophagosomes increased in  $H_2O_2$ -treated HaCaT cells, and the accumulation of LC-3, Beclin-1 and p62 was enhanced after  $H_2O_2$  treatment, as determined by Western blotting. These observations support that autophagy as well as apoptosis are important mechanisms of  $H_2O_2$ -mediated cytotoxicity in HaCaT cells. And, in the presence of loganin, these autophagy markers were remarkably reversed compared to cells treated with  $H_2O_2$  alone, showing that  $H_2O_2$ -induced HaCaT cell autophagy was clearly reduced by loganin supplementation. However, since autophagy has dual roles of pro-survival and pro-death depending on circumstances, additional mechanistic studies are required on how the alleviated effect of loganin on  $H_2O_2$ -induced autophagy affects the survival of HaCaT cells.

In the current study, we evaluated the efficacy of loganin on  $H_2O_2$ -mediated oxidative damage in HaCaT keratinocytes. Our results revealed that loganin visibly diminished cell cycle arrest at the G2/M phase, DNA damage, autophagy and apoptosis in  $H_2O_2$ -stimulated HaCaT cells, which was linked to its ability to suppress ROS accumulation. Additionally, the anti-apoptotic effect by loganin was a result of blockade of mitochondrial dysfunction, which correlated with inhibition of cytoplasmic release of cytochrome *c* due to inhibition of increased Bax/Bcl-2 ratio (Figure 7). This study provides a theoretical basis for the inhibitory mechanism of oxidative stress-mediated cellular damage of loganin and its application as a novel therapeutic agent to counteract oxidative stress-mediated skin diseases.

**Funding:** This research was supported by the National Research Foundation of Korea grant (2021R1A2C200954911) and Korea Basic Science Institute grant (2020R1A6C101A201) funded by the Korea government (MSIT).

**Conflict of Interest:** The authors have no conflicts of interest to disclose.

## References

- Gao X, Liu Y, An Z, Ni J. Active components and pharmacological effects of *Cornus officinalis*: Literature review. *Front Pharmacol*. 2021; 12:633447.
- Czerwińska ME, Melzig MF. *Cornus mas* and *Cornus officinalis* - Analogies and differences of two medicinal plants traditionally used. *Front Pharmacol*. 2018; 9:894.
- Huang J, Zhang Y, Dong L, Gao Q, Yin L, Quan H, Chen R, Fu X, Lin D. Ethnopharmacology, phytochemistry, and pharmacology of *Cornus officinalis* Sieb. et Zucc. *J Ethnopharmacol*. 2018; 213:280-301.
- Dinda B, Kyriakopoulos AM, Dinda S, Zoumpourlis V, Thomaidis NS, Velegriki A, Markopoulos C, Dinda M. *Cornus mas* L. (cornelian cherry), an important European and Asian traditional food and medicine: Ethnomedicine, phytochemistry and pharmacology for its commercial utilization in drug industry. *J Ethnopharmacol*. 2016; 193:670-690.
- Dong Y, Feng ZL, Chen HB, Wang FS, Lu JH. Corni Fructus: A review of chemical constituents and pharmacological activities. *Chin Med*. 2018; 13:34.
- Park E, Lee CG, Yun SH, Hwang S, Jeon H, Kim J, Yeo S, Jeong H, Yun SH, Jeong SY. Ameliorative effects of loganin on arthritis in chondrocytes and destabilization of the medial meniscus-induced animal model. *Pharmaceuticals (Basel)*. 2021; 14:135.
- Zhang J, Wang C, Kang K, Liu H, Liu X, Jia X, Yu K. Loganin attenuates septic acute renal injury with the participation of AKT and Nrf2/HO-1 signaling pathways. *Drug Des Devel Ther*. 2021; 15:501-513.
- Choi N, Yang G, Jang JH, Kang HC, Cho YY, Lee HS, Lee JY. Loganin alleviates gout inflammation by suppressing NLRP3 inflammasome activation and mitochondrial damage. *Molecules*. 2021; 26:1071.
- Wen H, Xing L, Sun K, Xiao C, Meng X, Yang J. Loganin attenuates intestinal injury in severely burned rats by regulating the toll-like receptor 4/NF- $\kappa$ B signaling pathway. *Exp Ther Med*. 2020; 20:591-598.
- Hu J, Zhou J, Wu J, Chen Q, Du W, Fu F, Yu H, Yao S, Jin H, Tong P, Chen D, Wu C, Ruan H. Loganin ameliorates cartilage degeneration and osteoarthritis development in an osteoarthritis mouse model through inhibition of NF- $\kappa$ B activity and pyroptosis in chondrocytes. *J Ethnopharmacol*. 2020; 247:112261.
- Yang Y, Gu Y, Zhao H, Zhang S. Loganin attenuates osteoarthritis in rats by inhibiting IL-1 $\beta$ -induced catabolism and apoptosis in chondrocytes via regulation of phosphatidylinositol 3-kinases (PI3K)/Akt. *Med Sci Monit*. 2019; 25:4159-4168.
- Xu YD, Cui C, Sun MF, Zhu YL, Chu M, Shi YW, Lin SL, Yang XS, Shen YQ. Neuroprotective effects of loganin on MPTP-induced Parkinson's disease mice: Neurochemistry, glial reaction and autophagy studies. *J Cell Biochem*. 2017; 118:3495-3510.
- Kim H, Youn K, Ahn MR, Kim OY, Jeong WS, Ho CT, Jun M. Neuroprotective effect of loganin against A $\beta$ <sub>25-35</sub>-induced injury via the NF- $\kappa$ B-dependent signaling pathway in PC12 cells. *Food Funct*. 2015; 6:1108-1116.
- Kwon SH, Kim JA, Hong SI, Jung YH, Kim HC, Lee SY, Jang CG. Loganin protects against hydrogen peroxide-induced apoptosis by inhibiting phosphorylation of JNK, p38, and ERK 1/2 MAPKs in SH-SY5Y cells. *Neurochem Int*. 2011; 58:533-541.
- Chen Y, Jiao N, Jiang M, Liu L, Zhu Y, Wu H, Chen J, Fu Y, Du Q, Xu H, Sun J. Loganin alleviates testicular damage and germ cell apoptosis induced by AGEs upon diabetes mellitus by suppressing the RAGE/p38MAPK/NF- $\kappa$ B pathway. *J Cell Mol Med*. 2020; 24:6083-6095.
- Cheng YC, Chu LW, Chen JY, Hsieh SL, Chang YC, Dai ZK, Wu BN. Loganin attenuates high glucose-induced Schwann cells pyroptosis by inhibiting ROS generation and NLRP3 inflammasome activation. *Cells*. 2020; 23:1948.
- Park C, Lee H, Kwon CY, Kim GY, Jeong JW, Kim SO, Choi SH, Jeong SJ, Noh JS, Choi YH. Loganin inhibits lipopolysaccharide-induced inflammation and oxidative response through the activation of the Nrf2/HO-1 signaling pathway in RAW264.7 macrophages. *Biol Pharm Bull*. 2021; 44:875-883.
- Benhar M. Oxidants, antioxidants and thiol redox switches in the control of regulated cell death pathways. *Antioxidants (Basel)*. 2020; 9:309.
- He L, He T, Farrar S, Ji L, Liu T, Ma X. Antioxidants maintain cellular redox homeostasis by elimination of reactive oxygen species. *Cell Physiol Biochem*. 2017; 44:532-553.
- Nakai K, Tsuruta D. What are reactive oxygen species, free radicals, and oxidative stress in skin diseases? *Int J Mol Sci*. 2021; 22:10799.
- Birch-Machin MA, Bowman A. Oxidative stress and ageing. *Br J Dermatol*. 2016; 175:S26-29.
- Paz ML, González Maglio DH, Weill FS, Bustamante J, Leoni J. Mitochondrial dysfunction and cellular stress progression after ultraviolet B irradiation in human keratinocytes. *Photodermatol Photoimmunol Photomed*. 2008; 24:115-122.
- Rizwan H, Pal S, Sabnam S, Pal A. High glucose augments ROS generation regulates mitochondrial dysfunction and apoptosis via stress signalling cascades in keratinocytes. *Life Sci*. 2020; 241:117148.
- Liu A, Zhang B, Zhao W, Tu Y, Wang Q, Li J. Catalpol ameliorates psoriasis-like phenotypes via SIRT1 mediated suppression of NF- $\kappa$ B and MAPKs signaling pathways. *Bioengineered*. 2021; 12:183-195.
- Shin D, Lee S, Huang YH, Lim HW, Lee Y, Jang K, Cho Y, Park SJ, Kim DD, Lim CJ. Protective properties of geniposide against UV-B-induced photooxidative stress in human dermal fibroblasts. *Pharm Biol*. 2018; 56:176-182.
- Ho JN, Lee YH, Park JS, Jun WJ, Kim HK, Hong BS, Shin DH, Cho HY. Protective effects of aucubin isolated from *Eucommia ulmoides* against UVB-induced oxidative stress in human skin fibroblasts. *Biol Pharm Bull*. 2005; 28:1244-1248.
- Kim MY, Choi YW, Hwang HS. Regulatory effect on skin differentiation by mevastatin in psoriasis model using TNF- $\alpha$  and IL-17 induced HaCaT cells. *Biotechnol Bioprocess Eng*. 2021; 26:348-358.
- Sim KH, Shu MS, Kim S, Kim JY, Choi BY, Lee YJ. Cilostazol induces apoptosis and inhibits proliferation of hepatocellular carcinoma cells by activating AMPK. *Biotechnol Bioprocess Eng*. 2021; 26:776-785.
- Liu Z, Ouyang G, Lu W, Zhang H. Long non-coding RNA HOTAIR promotes hepatocellular carcinoma progression by regulating miR-526b-3p/DHX33 axis. *Genes Genomics*. 2021; 43:857-868.

30. Lee H, Kim DH, Kim JH, Park SK, Jeong JW, Kim MY, Hong SH, Song KS, Kim GY, Hyun JW, Choi YH. Urban aerosol particulate matter promotes necrosis and autophagy *via* reactive oxygen species-mediated cellular disorders that are accompanied by cell cycle arrest in retinal pigment epithelial cells. *Antioxidants (Basel)*. 2021; 10:149.
31. Noh Y, Ahn JH, Lee JW, Hong J, Lee TK, Kim B, Kim SS, Won MH. Brain Factor-7<sup>®</sup> improves learning and memory deficits and attenuates ischemic brain damage by reduction of ROS generation in stroke *in vivo* and *in vitro*. *Lab Anim Res*. 2020; 36:24.
32. Volobaev VP, Serdyukova ES, Kalyuzhnaya EE, Schetnikova EA, Korotkova AD, Naik AA, Bach SN, Prosekov AY, Larionov AV. Investigation of the genotoxic effects of fluoride on a bone tissue model. *Toxicol Res*. 2020; 36:337-342.
33. Raavi V, Perumal V, Paul SFD. Potential application of  $\gamma$ -H2AX as a biodosimetry tool for radiation triage. *Mutat Res Rev Mutat Res*. 2021; 787:108350.
34. Choi MJ, Mukherjee S, Yun JW. Loss of ADAMTS15 promotes browning in 3T3-L1 white adipocytes *via* activation of  $\beta$ 3-adrenergic receptor. *Biotechnol Bioprocess Eng*. 2021; 26:188-200.
35. Kim JH, Baek JI, Lee IK, Kim UK, Kim YR, Lee KY. Protective effect of berberine chloride against cisplatin-induced ototoxicity. *Genes Genomics*. 2022; 44:1-7.
36. Kim SY, Park C, Kim MY, Ji SY, Hwangbo H, Lee H, Hong SH, Han MH, Jeong JW, Kim GY, Son CG, Cheong J, Choi YH. ROS-mediated anti-tumor effect of Coptidis Rhizoma against human hepatocellular carcinoma Hep3B cells and xenografts. *Int J Mol Sci*. 2021; 22:4797.
37. Emmert H, Culley J, Brunton VG. Inhibition of cyclin-dependent kinase activity exacerbates H<sub>2</sub>O<sub>2</sub>-induced DNA damage in Kindler syndrome keratinocytes. *Exp Dermatol*. 2019; 28:1074-1078.
38. Thorn T, Gniadecki R, Petersen AB, Vicanova J, Wulf HC. Differences in activation of G2/M checkpoint in keratinocytes after genotoxic stress induced by hydrogen peroxide and ultraviolet A radiation. *Free Radic Res*. 2001; 35:405-416.
39. Panieri E, Gogvadze V, Norberg E, Venkatesh R, Orrenius S, Zhivotovsky B. Reactive oxygen species generated in different compartments induce cell death, survival, or senescence. *Free Radic Biol Med*. 2013; 57:176-187.
40. Park C, Lee H, Noh JS, Jin CY, Kim GY, Hyun JW, Leem SH, Choi YH. Hemistepsin A protects human keratinocytes against hydrogen peroxide-induced oxidative stress through activation of the Nrf2/HO-1 signaling pathway. *Arch Biochem Biophys*. 2020; 691:108512.
41. Brillo V, Chierogato L, Leanza L, Muccioli S, Costa R. Mitochondrial dynamics, ROS, and cell signaling: A blended overview. *Life (Basel)*. 2021; 11:332.
42. Jiang Q, Yin J, Chen J, Ma X, Wu M, Liu G, Yao K, Tan B, Yin Y. Mitochondria-targeted antioxidants: A step towards disease treatment. *Oxid Med Cell Longev*. 2020; 2020:8837893.
43. Cordelli E, Bignami M, Pacchierotti F. Comet assay: A versatile but complex tool in genotoxicity testing. *Toxicol Res (Camb)*. 2021; 10:68-78.
44. Park C, Cha HJ, Hong SH, Kim GY, Kim S, Kim HS, Kim BW, Jeon YJ, Choi YH. Protective effect of phloroglucinol on oxidative stress-induced DNA damage and apoptosis through activation of the Nrf2/HO-1 signaling pathway in HaCaT human keratinocytes. *Mar Drugs*. 2019; 17:225.
45. Shim JH, Kim KH, Cho YS, Choi HS, Song EY, Myung PK, Kang JS, Suh SK, Park SN, Yoon DY. Protective effect of oxidative stress in HaCaT keratinocytes expressing E7 oncogene. *Amino Acids*. 2008; 34:135-141.
46. Dadsena S, King LE, García-Sáez AJ. Apoptosis regulation at the mitochondria membrane level. *Biochim Biophys Acta Biomembr*. 2021; 1863:183716.
47. Xiong S, Mu T, Wang G, Jiang X. Mitochondria-mediated apoptosis in mammals. *Protein Cell*. 2014; 5:737-749.
48. Lyamzaev KG, Knorre DA, Chernyak BV. Mitoptosis, twenty years after. *Biochemistry (Mosc)*. 2020; 85:1484-1498.
49. Kaminsky VO, Zhivotovsky B. Free radicals in cross talk between autophagy and apoptosis. *Antioxid Redox Signal*. 2014; 21:86-102.
50. Fidrus E, Hegedús C, Janka EA, Paragh G, Emri G, Remenyik É. Inhibitors of nucleotide excision repair decrease UVB-induced mutagenesis - An *in vitro* study. *Int J Mol Sci*. 2021; 22:1638.
51. Piao MJ, Ahn MJ, Kang KA, Ryu YS, Hyun YJ, Shilnikova K, Zhen AX, Jeong JW, Choi YH, Kang HK, Koh YS, Hyun JW. Particulate matter 2.5 damages skin cells by inducing oxidative stress, subcellular organelle dysfunction, and apoptosis. *Arch Toxicol*. 2018; 92:2077-2091.
52. Trelford CB, Di Guglielmo GM. Molecular mechanisms of mammalian autophagy. *Biochem J*. 2021; 478:3395-3421.
53. Condello M, Pellegrini E, Caraglia M, Meschini S. Targeting autophagy to overcome human diseases. *Int J Mol Sci*. 2019; 20:725.
54. Sánchez-Martín P, Komatsu M. Physiological stress response by selective autophagy. *J Mol Biol*. 2020; 432:53-62.
55. Zhao YG, Zhang H. Core autophagy genes and human diseases. *Curr Opin Cell Biol*. 2019; 61:117-125.
56. Xiang H, Zhang J, Lin C, Zhang L, Liu B, Ouyang L. Targeting autophagy-related protein kinases for potential therapeutic purpose. *Acta Pharm Sin B*. 2020; 10:569-581.
57. Tran S, Fairlie WD, Lee EF. BECLIN1: Protein structure, function and regulation. *Cells*. 2021; 10:1522.
58. Xu HD, Qin ZH. Beclin 1, Bcl-2 and autophagy. *Adv Exp Med Biol*. 2019; 1206:109-126.
59. Takahashi D, Arimoto H. Selective autophagy as the basis of autophagy-based degraders. *Cell Chem Biol*. 2021; 28:1061-1071.
60. Liu WJ, Ye L, Huang WF, Guo LJ, Xu ZG, Wu HL, Yang C, Liu HF. p62 links the autophagy pathway and the ubiquitin-proteasome system upon ubiquitinated protein degradation. *Cell Mol Biol Lett*. 2016; 21:29.

Received March 14, 2022; Revised March 29, 2022; Accepted May 31, 2022.

\*Address correspondence to:

Yung Hyun Choi, Department of Biochemistry, College of Korean Medicine, Dong-eui University, Busan 47227, Republic of Korea.

E-mail: choiyh@deu.ac.kr

Released online in J-STAGE as advance publication June 10, 2022.